

4-17-1987

A Calculation Method for Quantitative X-Ray Microanalysis for Microparticle Specimens by Monte Carlo Simulation

Yen-cai Ho
Shanghai Institute of Ceramics

Jia-guang Chen
Shanghai Baoshan Steel Works

Min Hu
Shanghai Institute of Ceramics

Xin-lei Wang
Shanghai Institute of Ceramics

Follow this and additional works at: <https://digitalcommons.usu.edu/microscopy>



Part of the [Life Sciences Commons](#)

Recommended Citation

Ho, Yen-cai; Chen, Jia-guang; Hu, Min; and Wang, Xin-lei (1987) "A Calculation Method for Quantitative X-Ray Microanalysis for Microparticle Specimens by Monte Carlo Simulation," *Scanning Microscopy*: Vol. 1 : No. 3 , Article 8.

Available at: <https://digitalcommons.usu.edu/microscopy/vol1/iss3/8>

This Article is brought to you for free and open access by the Western Dairy Center at DigitalCommons@USU. It has been accepted for inclusion in Scanning Microscopy by an authorized administrator of DigitalCommons@USU. For more information, please contact digitalcommons@usu.edu.



A CALCULATION METHOD FOR QUANTITATIVE X-RAY MICROANALYSIS
FOR MICROPARTICLE SPECIMENS BY MONTE CARLO SIMULATION

Yen-cai Ho^{1*}, Jia-guang Chen², Min Hu¹ and Xin-lei Wang¹

¹Shanghai Institute of Ceramics, Academia Sinica
865 Chang-ning Road, Shanghai 200050, China

²Research Department, Shanghai Baoshan Steel Works
Baoshan, Shanghai, China

(Received for publication December 22, 1986, and in revised form April 17, 1987)

Abstract

A calculation method for quantitative X-ray microanalysis (QXMA) for microparticle specimens of a compound with various shapes is proposed in this paper. On the basis of a simplified physical model, the scattering of electrons in particles is calculated by Monte Carlo simulation. We have derived a series of evaluation formulae of the absorption and fluorescence of characteristic X-rays for the particles with regular shapes. With the use of these theories, along with an iteration calculation, compositions of microparticle specimens can be obtained from the measured X-ray intensity ratios. In order to examine the reliability of the method, a large number of electron probe experiments and analysis calculations were carried out for the microparticle specimens of a variety of geometric shapes, dimensions and compositions. Agreement of calculated concentrations using our method with known compositions of the analyzed particle specimens is fairly good. In practical work, calculation formulae for particle specimens with irregular shapes can be replaced by those of particles with approximate regular shapes.

KEY WORDS: Microparticle, quantitative X-ray microanalysis, Electron scattering, Monte Carlo simulation.

*Address for correspondence:
865 Chang-ning Road,
Shanghai 200050, China

Phone No. 522470

Introduction

In quantitative analysis of individual microparticles, Armstrong¹ has developed a series of theoretical corrections for particles of a variety of idealized geometric shapes and an accurate experimental method. In the present paper, a new QXMA method for microparticles based on stricter theories and Monte Carlo technique is introduced. This approach is directly applicable to the electron probe analysis of oxide particles, and can be easily extended to QXMA of particle specimens with arbitrary shapes. The flow chart of the calculating program of our method is given here.

Principle

Calculation of electron scattering and X-ray intensity in alloy particles of arbitrary shapes

When the electron beam with a certain energy bombards an alloy particle (Fig. 1), the spatial positions and energy distribution of the electrons and the X-ray production in the specimen will be decided by the elastic and inelastic scattering of the electrons. The electron scattering, production, absorption and fluorescence of characteristic X-rays are physical processes, which cannot be treated by using conventional methods, such as the ZAF procedures.

The calculation procedures developed by us are as follows:

1) Simulation of incident electron beam. An ideal focused electron beam has a Gaussian intensity distribution along its diameter, and the diameter of the circle containing 80 percent of the current is considered as the diameter^{8,2}. Based on these considerations, the electron distribution of incident beam can be simulated by Gaussian random number (Fig. 2).

2) Step length of electron scattering. In the present study, we use a simplified physical model to describe the scattering processes of electrons in a target. In this model, the step length of electron scattering is fixed, and Rutherford cross section in its simplest form is expressed. The calculation approach was established by Curgenvén and Duncumb³, and has been extensively applied to QXMA^{6,7}. For the energy range of electron beam microanalysis, the differences

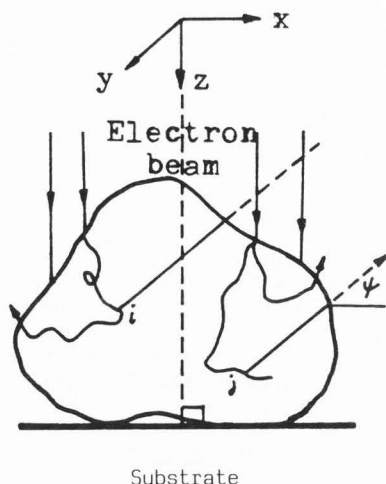


Fig. 1. Electron and X-ray excitation in a particle.



Fig. 2. Electron distribution simulated by Gaussian random number.

between calculated results (such as the back-scatter coefficient, η , and the depth distribution function of X-rays) using the simplified model and 'single scattering model' are very small.

Bethe's energy loss equation for a compound is:

$$\frac{dE}{dps} = - \frac{2\pi e^4 N}{E} \cdot \sum_i C_i \frac{Z_i}{A_i} \ln \left(\frac{1.166E}{J_i} \right), \quad (1)$$

where N is Avogadro's number, Z_i and A_i are the atomic number and atomic weight of i atoms, respectively, and J_i is the mean ionization potential.

The total electron path length ρs_m is calculated by formula (1). We take 1% of Bethe range ρs_m as the step length of electron scattering.

3) Angular scattering of electrons. Let $\sigma(\theta)$ be the Rutherford cross section, the total cross section σ_i is obtained by integrating $\sigma(\theta)$ over the whole solid angle 4π

$$\sigma_i = \left(\frac{Z_i e^2}{2E} \right)^2 \cdot \frac{2\pi}{\alpha_i (1 + \alpha_i)}, \quad (2)$$

where α_i is the screening parameter of i atoms. The relative total section of i atoms in an alloy is:

$$\sigma_{it} = \frac{C_i}{A_i} \sigma_i.$$

The normalized value:

$$P_i = \frac{\sigma_{it}}{\sum_i \sigma_{it}}, \quad (3)$$

expresses the probability that an electron is scattering by i atoms.

The angular distribution of electrons is determined by the Rutherford scattering equation:

$$\cot \left(\frac{\theta}{2} \right) = \frac{P \cdot E}{0.0072 \cdot Z}, \quad (4)$$

in which P is the impact parameter, $P = P_0(R)^{1/2}$. R is uniform random number in the range 0-1, we take $0.874 \cdot Z^{0.4} / E_0$ as the maximum collision parameter P_0 . E_0 is the primary energy of incident electrons.

4) Calculation of X-ray intensity. Suppose that $f(x, y, z)$ is a surface function of the particle under the electron beam with Gaussian distribution, the electron trajectories in the particle can be evaluated by Monte Carlo simulation from the origin of the primary coordinate $f(x_0, y_0, z_0)$ until the electron leaves the particle. Thus the spatial coordinates and the energy distribution of incident electrons in an alloy particle are obtained.

Considering the absorption and fluorescence of characteristic X-rays, the general equation of the emitted intensity of X-rays of element i in specimens with arbitrary shapes:

$$I_{A.F.i} = K_F \cdot \iiint \phi_i \exp(-\mu_i \rho s(x, y, z)) dx dy dz, \quad (5)$$

where ϕ_i is the probability of a characteristic X-ray of element i excited by incident electrons in particles, μ_i is the mass absorption coefficient of the sample for the radiation of the exciting element i , $s(x, y, z)$ is the absorption path function of X-ray photons, and K_F is the fluorescence coefficient.

The X-ray intensity emitted from the standard sample of pure element i is calculated from the expression:

$$I_{S.i} = \int_0^\infty \phi(\rho z) \exp(-\mu \rho z \csc \psi) dz, \quad (6)$$

in which μ is the m.a.c. of the standard sample, ρz is the mass depth of X-ray photons, and ψ is the X-ray take-off angle, i.e., the angle between the take-off direction and the plane of substrates for particle specimens.

In calculating $\phi(\rho z)$ function, the number of X-rays is determined using the ionization cross-section $Q(U)$. The expression is:

$$Q(U) = (\text{const}/U)\ln U$$

where U is the overvoltage E/E_c , E_c being the critical excitation potential of the X-ray line of interest.

The X-ray intensity ratio is given by:

$$k_i = \frac{I_{A.F.i}}{I_{S.i}} \quad (7)$$

Calculation formulae of $s(x,y,z)$ and k_f

It is impossible to derive strictly the absorption path function $s(x,y,z)$ in eq.(5) for particle specimens with arbitrary shapes. Based on physical fact, we have assumed that the X-ray photons are concentrated on the axis of the incident electron beam, and therefore derive the calculation formulae of the function $s(x,y,z)$ for the particles with the regular shapes of cuboid, cylinder, elliptic cylinder, spheroid and elliptic spheroid⁴.

For cuboid (length=a, width=b, height=c) or elliptic cylinder (long axis=a/2, short axis=b/2, height=c):

$$s(x,y,z)=s(z)=z/\sin\psi, \text{ at } z < \frac{a+b}{4} \cdot \text{tg}\psi,$$

$$\text{and } s(z)=\frac{a+b}{4\cos\psi}, \text{ at } z \geq \frac{a+b}{4} \cdot \text{tg}\psi.$$

For spheroid (diameter 2r):

$$s(z)=(r^2-(r-z)^2 \cdot \cos^2\psi)^{1/2} - (r-z)\sin\psi.$$

For elliptic spheroid (three axes are respectively, a, b and c), let A be $(a+b)^2/4$, B be $(c-z)$, then:

$$s(z)=(((2A \cdot B \cdot \text{tg}\psi)^2 - 4(c^2 + A \cdot \text{tg}^2\psi)(A \cdot B^2 - A \cdot c^2))^{1/2} - 2A \cdot B \cdot \text{tg}\psi) / 2(c^2 + A \cdot \text{tg}^2\psi).$$

It is similarly impossible to exactly calculate the fluorescence coefficient k_f in particles of arbitrary shapes.

Considering the axial symmetry of primary characteristic X-ray photons and excited fluorescence photons, we have assumed that: 1) X-ray photons have a spherical distribution in specimens and the whole intensities of primary X-rays are concentrated on the centre of the X-ray photon spheroid. 2) The excited fluorescence photons concentrate on the centre of the secondary X-ray photons.

The fluorescence intensity formula for the particles of symmetric shapes is derived from these assumptions (deriving process in the Appendix):

$$\frac{I_f}{I_i} = \frac{1}{2} C_j \frac{\mu_j^i}{\mu_j} \cdot \frac{r_i^{-1}}{r_i} \omega(j) \frac{A_i}{A_j} \left(\frac{u_j^{-1}}{u_i^{-1}} \right)^{1.67} \cdot e^{-\mu_i \rho r} \cdot \int_0^\pi (e^{-\mu_j r_1(\varphi)} + e^{-\mu_j r_2(\varphi)}) \cdot \sin\varphi d\varphi,$$

where C_j is the concentration of element j, μ_j^i is the m.a.c. of element i for j radiation, μ_j is the m.a.c. of a sample for i radiation, r_i the absorption edge jump ratio of element i, $\omega(j)$ the fluorescence yield of i radiation, u_i is the overvoltage ratio, r is the absorption path of fluorescence photons from the centre of the secondary photons to the surface of a particle, $f_{1,2}(\varphi)$ is the integrated variate function.

There is a good agreement between the fluorescence coefficients calculated using our equation and those obtained using the ZAF method for thick polished specimens.

Calculation of alloy particle concentration C_i using Monte Carlo iteration

Taking the normalized values of the measured X-ray intensity ratio Mk_i as the first approximate values C_i^1 of the particle composition, the electron scattering processes in the particle sample with the assumed composition C_i^1 are calculated by Monte Carlo simulation, the emitted intensity ratio k_i^1 is simultaneously determined by using the corrections of the absorption and fluorescence of characteristic X-rays mentioned above.

Usually, there is a certain difference between k_i^1 and Mk_i , it may be written:

$$\Delta k_i^1 = k_i^1 - Mk_i \quad (8)$$

Since the X-ray intensity emitted from element i increases with a rise of the concentration of element i in specimens, the second approximate composition C_i^2 is given by:

$$C_i^2 = \frac{C_i^1 - \Delta k_i^1}{\sum_1 (C_i^1 - \Delta k_i^1)} \quad (9)$$

Repeating the calculation process above mentioned until the nth iteration, for a given arbitrary small quantity ϵ , if:

$$|C_i^n - C_i^{n-1}| < \epsilon,$$

then C_i^n is the concentration of the analyzed particle specimen.

Iteration program by Monte Carlo simulation

We have made the Monte Carlo calculation program using WANG VS BASIC language. Figure 3 shows the flow chart of a Monte Carlo program. The program can be applied to the calculations of QXMA for alloy microparticle specimens containing less than eight elements. The data files of atomic number, atomic weight, density, X-ray mass

attenuation coefficient and the other physical constants of 72 elements from beryllium to uranium have been established in this program, and the calculation formulae of particle specimens with the regular shapes of cube, cuboid, cylinder, spheroid, elliptic cylinder and elliptic spheroid are given here.

The calculation formulae of a particle specimen of irregular shape may be replaced by that of the most approximate regular shape. In our work, the correction calculation for thin film samples is seen as a particular example of a cuboid which has large enough size so that more than 50 μm in its length, width, and height represents the thickness of film samples. Therefore, the calculation formulae of QXMA for cuboids are quite suitable for thin films and thick polished specimens.

In this Monte Carlo program, if we let the value ϵ be 0.005, usually, the iteration calculation converges quite rapidly.

EPQA experiments

In order to examine the reliability of the calculation method proposed in this paper, we have carried out a large number of experiments of the electron probe quantitative analysis (EPQA) for the Fe-Cr-Ni alloy standard thick specimen, the Fe-Cr-Ni-Co-Si-B alloy spherical particles, the γ' alloy particles of cube and cuboid shapes and the PbS crystal particles with shapes approximate cube and cuboid.

Sample preparation and experimental conditions

The Fe-Cr-Ni standard specimen was provided by National Bureau of Standards (U.S.), it is the standard for QXMA experiment. The alloy spherical particles were prepared by using the technique of argon protection, the γ' alloy particles were made by using the electrolysis extraction method from the block alloy sample.

The experimental conditions for the alloy standard specimen and the particle specimens are indicated in tables 1 and 2. Figs. 4 and 5 are the micrographs of the spherical particle and the PbS particle.

Results and Discussion

The calculated compositions using our method and the ZAF correction method for the Fe-Cr-Ni standard specimen are given in table 1. Agreement of the results calculated using the two methods is fairly good. The results analyzed by using our method for the spherical particles and the PbS particles are in agreement with the true concentrations of these specimens, though some systematic errors appear here. However, there are some deviations between the calculated results using the ZAF procedure and the true concentrations for the particle specimens (table 2), and the smaller the size of particles, the greater is the calculated deviation.

The emphasis of this paper is to propose a series of theories for the QXMA of microparticles. However, there is much research work to be done in the experimental technique of the QXMA of micro-

particle specimens. We have analyzed over 200 particles of a variety of materials having known compositions and shapes, and have therefore obtained some experimental rules. Those will be discussed in another paper.

This method can be easily extended to the QXMA of oxide particle specimens of arbitrary shapes.

EPQA experiments were carried out in JCXA-733 Probe, Monte Carlo simulation was calculated on WANG VS 100 Computer.

Appendix

The solid angle subtended by the annulus in Fig. 6 is $2\pi \sin\varphi d\varphi$. Considering the mass attenuation of characteristic X-ray I_j in the radiation process, then the absorbed I_j radiation by the thin annulus is $(\frac{1}{2} I_j \sin\varphi d\varphi) e^{-\mu_j \rho z \sec\varphi} (\mu_i \rho dz \sec\varphi)$. Let ϵ be the rate of fluorescence conversion of element i , counting the absorption process of fluorescence in the particle, hence, the excited fluorescence intensity in the annulus:

$$\begin{aligned} \Delta I_f &= \epsilon \left(\frac{1}{2} I_j \sin\varphi d\varphi \right) (\mu_i \rho dz \sec\varphi) e^{-\mu_j \rho z \sec\varphi} e^{-\mu_i \rho r} \\ &= \frac{1}{2} \epsilon I_j \mu_j \text{tg}\varphi e^{-\mu_j \rho z \sec\varphi} e^{-\mu_i \rho r} d\varphi dz. \end{aligned} \quad (10)$$

Integrating eq.(10) for the lower part and the upper part of plane EF of the particle, we arrive at the total fluorescence intensity in the particle:

$$I_f = I_{f1} + I_{f2}. \quad (11)$$

Integration of the lower part

$$I_{f1} = \frac{1}{2} \epsilon I_j \mu_j \int_0^{\frac{\pi}{2}} \int_0^{O'D} e^{-\mu_j \rho z \sec\varphi} e^{-\mu_i \rho r} \text{tg}\varphi d\varphi dz. \quad (12)$$

The integration limit along coordinate Z , $O'D = O'A \cdot \cos\varphi$. For specimens with arbitrary shapes, $O'A$ versus angle φ and horizontal position angle θ , i.e.,

$$O'A = f1(\varphi, \theta).$$

For the particle specimens with symmetric shapes,

$$f1(\varphi, \theta) = f1(\varphi).$$

$$O'D = f1(\varphi) \cdot \cos\varphi.$$

Hence,

$$\begin{aligned} I_{f1} &= \frac{1}{2} \epsilon I_j \mu_j \int_0^{\frac{\pi}{2}} e^{-\mu_i \rho r} \text{tg}\varphi d\varphi \\ &\quad \cdot \int_0^{f1(\varphi) \cos\varphi} e^{-\mu_j \rho z \sec\varphi} dz \end{aligned}$$

$$\begin{aligned}
 &= \frac{1}{2} \mathcal{E} I_j \mu_j \int_0^{\frac{\pi}{2}} e^{-\mu_i \rho r} \operatorname{tg} \varphi d\varphi \\
 &\cdot \int_0^{\frac{\pi}{2}} \frac{f1(\varphi) \cos \varphi_1}{-\mu_j \rho \sec \varphi} e^{-\mu_j \rho z \sec \varphi} d(-\mu_j \rho z \sec \varphi) \\
 &= \frac{1}{2} \mathcal{E} I_j e^{-\mu_i \rho r} \left(1 - \int_0^{\frac{\pi}{2}} e^{-\mu_j \rho f1(\varphi)} \sin \varphi d\varphi \right). \\
 I_{f2} &= \frac{1}{2} \mathcal{E} I_j e^{-\mu_i \rho r} \left(1 - \int_0^{\frac{\pi}{2}} e^{-\mu_j \rho f2(\varphi)} \sin \varphi d\varphi \right). \\
 I_f &= \frac{1}{2} \mathcal{E} I_j e^{-\mu_i \rho r} \left(2 - \int_0^{\frac{\pi}{2}} (e^{-\mu_j \rho f1(\varphi)} + e^{-\mu_j \rho f2(\varphi)}) \sin \varphi d\varphi \right). \quad (13)
 \end{aligned}$$

The product of the conversion efficiency factor \mathcal{E} and the radiation I_j is expressed as follows:

$$\mathcal{E} I_j = C_j \frac{\mu_j^i}{\mu_j} \cdot \frac{r_i - 1}{r_i} \omega(j) \frac{A_i}{A_j} \left(\frac{u_j - 1}{u_i - 1} \right)^{1.67} I_i \quad (14)$$

The complete fluorescence formula is thus:

$$\begin{aligned}
 \frac{I_f}{I_i} &= \frac{1}{2} C_j \frac{\mu_j^i}{\mu_j} \cdot \frac{r_i - 1}{r_i} \omega(j) \frac{A_i}{A_j} \left(\frac{u_j - 1}{u_i - 1} \right)^{1.67} \cdot e^{-\mu_i \rho r} \cdot \left(2 - \int_0^{\frac{\pi}{2}} (e^{-\mu_j \rho f1(\varphi)} + e^{-\mu_j \rho f2(\varphi)}) \sin \varphi d\varphi \right). \quad (15)
 \end{aligned}$$

For spherical particle specimens, $f1(\varphi) = f2(\varphi) = r$ (radius), then:

$$\begin{aligned}
 \frac{I_f}{I_i} &= C_j \frac{\mu_j^i}{\mu_j} \cdot \frac{r_i - 1}{r_i} \omega(j) \frac{A_i}{A_j} \left(\frac{u_j - 1}{u_i - 1} \right)^{1.67} e^{-\mu_i \rho r} (1 - e^{-\mu_j \rho r}). \quad (16)
 \end{aligned}$$

References

1. Armstrong, J. T. (1978). Method of quantitative analysis of individual microparticles with electron beam instrument, Scanning Electron Microsc. 1978; I:455-467.
2. Broers, A. N., (1973). High-resolution scanning electron microscopy of surfaces, In: Microprobe Analysis, Anderson CA (ed.), Wiley, New York, 88.
3. Curgenvén L, Duncumb P. (1971). Simulation of electron trajectories in a solid target by a simple Monte Carlo technique, Tube Investments Research Report 303.

4. Ho, Y. C., (1984). Formulae for the absorption paths of X-ray photons in the particle of some regular shapes, Kexue Tongbao, Beijing, 29, 177.

5. Ho, Y. C., Huang Y. H. (1982). Calculation of transmission coefficients of electrons and the depth of X-ray production in solids by Monte Carlo simulation, J. Physics (in Chinese), 11, 537.

6. Ho, Y. C., Huang Y. H. (1982). A simple method for electron probe determination of thickness of thin films by Monte Carlo simulation, Scanning Electron Microsc. 1982; II: 559-562.

7. Love, G., Cox M. G. C., Scott V. D. (1977). A simple Monte Carlo method for simulating electron-solid interactions and its application to electron probe microanalysis, J. Phys. D, 10, 7.

8. Wells, O. C. (1974). Scanning Electron Microscopy, McGraw Hill, New York, 71.

Discussion with Reviewers

P. Statham: What is the average computation time for correction of a single particle?

Authors: The average computation time is about ten minutes in central processor unit (CPU) on WANG VS 100 Computer for correction of a single particle specimen of a compound.

P. Statham: Have you studied the propagation of errors through this procedure so that it is possible to quantify the likely error if the particle shape is incorrectly specified?

Authors: The error of this correction method mainly results from two aspects: (a) the physical model calculating electron scattering and X-ray excitation, and (b) the correction formulae of the absorption and fluorescence of X-rays. Usually, the error of calculated X-ray distribution function $\phi(\rho z)$ using the simplified model is smaller than 3%⁷ at 15-30 keV except heavy element. Since the absorption and fluorescence effects for particle specimens are very small (<1%), the error due to formulae of the absorption and fluorescence can be ignored. Consequently, the error of this calculation method is lower than 3%. However, a very important problem in particle analysis is the error from EPQA experiments: the smaller the dimension of particles, the larger is the error. When the particles are smaller in area than the diameter of the electron beam, X-ray intensities are very low so that there is a large error due to the detection limits of the X-ray spectrometer. The particle sizes (or the diameter of beams) and shapes should be carefully measured, otherwise, considerable errors can result. For example, we replaced 0.2 μm (particle size) by 0.22 μm in calculating the compositions of PbS particle (table 2), the concentrations obtained are: S, 0.139; Pb, 0.860. Thus there is 1.4% absolute error.

R. Sartore: With respect to the application of your correction calculations to thin film samples, you mentioned the use of a cuboid structure that is more than 50 microns on a side as a good example.

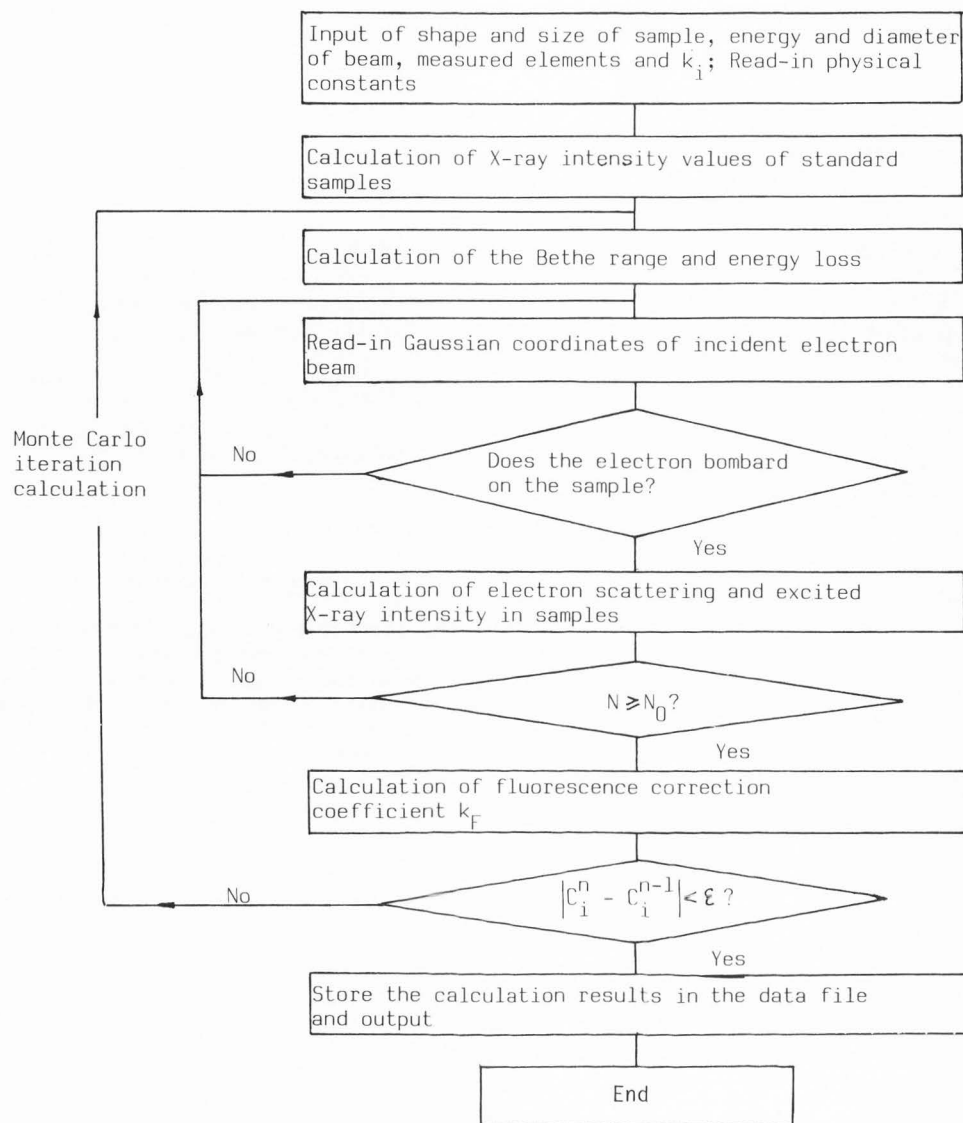


Fig. 3. Schematic flow chart of iteration calculation by Monte Carlo simulation for QXMA of particles of arbitrary shapes. N_0 is the total simulated electron number.

What is the range of thin film thicknesses, to which your calculations would be applicable? Would your correction calculations be applicable to film thickness in the 1 micron range?

Authors: In our method, the thin film specimens are treated as the peculiar cuboid ones with large size (more than $50 \mu\text{m}$ in its length and width) and the height of the cuboid as the thickness of film specimens. In the energy range 10-50 keV of EPQA, this method can be applied to the correction calculations for thin films with thickness range of hundreds \AA to several μm .

P.Statham: How do your results on particles compare with those for standard ZAF but with normalization?

Authors: The results calculated using our method and the standard ZAF method (with normalization) are given in table 2 for spherical particles and PbS particles. It is clear that the smaller the size of a particle, the larger are the differences between the compositions calculated using the ZAF procedure and the true concentrations. The differences are small for spherical particles with a diameter of $1.8 \mu\text{m}$.

P. Statham: Have you experienced any problems with convergence with your iteration technique?

Authors: Yes, if the measured errors of X-ray intensity ratios Mk_i are large, there will be a problem with convergence.



Fig. 4. Alloy spherical particle micrography. Diameter, 1.8 μm ; substrate, polished graphite piece.

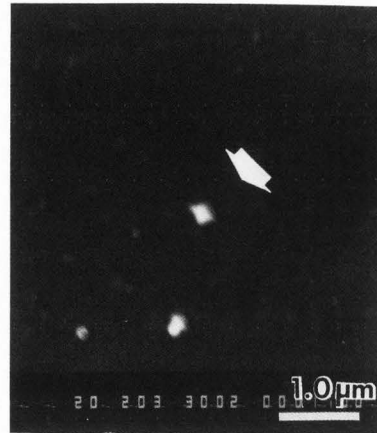


Fig. 5. PbS particle micrography. Shape, approximate cube; dimension, 0.22x0.22x0.22 μm ; substrate, polished graphite piece.

Voltage (kV)	Element	Measured K values	Calculated compositions by M.C. method	Calculated compositions by ZAF method
20	Cr	0.211	0.180	0.185
	Fe	0.694	0.708	0.709
	Ni	0.095	0.105	0.104
25	Cr	0.213	0.180	0.185
	Fe	0.685	0.717	0.711
	Ni	0.089	0.105	0.104
30	Cr	0.216	0.184	0.187
	Fe	0.672	0.717	0.709
	Ni	0.085	0.105	0.104
35	Cr	0.216	0.182	0.187
	Fe	0.664	0.704	0.714
	Ni	0.081	0.107	0.105

Table 1. Comparison between the results calculated using Monte Carlo method and ZAF method for the Fe-Cr-Ni standard. Actual conc. Fe 0.696-0.724, Cr 0.176-0.186, Ni 0.107-0.111. Beam current, 1×10^{-8} A.

P. Statham: The fluorescence correction is likely to be small yet demands a lot of computation. Do your results suggest any criteria for deciding when fluorescence enhancement can safely be ignored?

Authors: We have calculated the fluorescence coefficients for the Fe-Cr-Ni-Co-Si-B alloy spherical particles of different sizes. The results show that fluorescence effects can be ignored when the particles are smaller than 1 μm .

J.D.Brown: A different approach is generally required in particle analysis depending on whether

the particles are larger than the beam size and thicker than the electron penetration depth or smaller than the beam size and thinner than the electron penetration depth. Does the method described apply to both cases and if so what changes or precautions are necessary?

Authors: The method described can be applied to the correction calculations of both the cases you mention, and there is no need of making any change. However, it is necessary to perform the EPQA experiments carefully for the particle specimens which are smaller than the beam size or thinner than the electron penetration depth.

Table 2. The results calculated using Monte Carlo method for the spherical particle specimen and the PbS particle specimens of cuboid and cube. Experimental conditions: spheroid (Fig. 4), voltage 15 kV, beam diameter $0.2 \mu\text{m}$, beam current 1×10^{-8} A; cuboid, 20 kV, $0.15 \mu\text{m}$, 1×10^{-8} A; cube(1) 20 kV, $0.15 \mu\text{m}$, 1×10^{-8} A; cube(2), 20 kV, $0.3 \mu\text{m}$, 1×10^{-8} A. X-ray lines used: B, Si, Cr, Fe, Co, Ni and S, k_{α} ; Pb, L_{α} . *The calculated values by ZAF method are normalized.

Particle dimension	Element	Measured k values	Calculated compo. by MC method	Calculated compo. by ZAF method*	Actual compo.
Spheroid diameter: $1.8 \mu\text{m}$	B	0.004	0.021	0.032	0.027
	Si	0.020	0.045	0.033	0.035
	Cr	0.139	0.163	0.147	0.155
	Fe	0.045	0.051	0.046	0.052
	Co	0.088	0.097	0.103	0.101
	Ni	0.566	0.623	0.640	0.626
PbS cuboid $1.7 \times 0.95 \times 0.95 \mu\text{m}$	S	0.071	0.151	0.087	0.134
	Pb	0.617	0.849	0.912	0.866
PbS cube(1) $1 \times 1 \times 1 \mu\text{m}$	S	0.069	0.155	0.089	0.134
	Pb	0.584	0.845	0.910	0.866
PbS cube(2) $0.2 \times 0.2 \times 0.2 \mu\text{m}$	S	0.008	0.153	0.082	0.134
	Pb	0.075	0.847	0.918	0.866

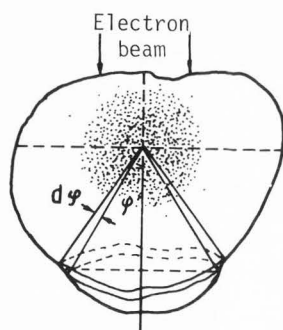


Fig. 6. Schematic diagram of exciting fluorescence in specimens with arbitrary shapes.